processes

MDPI

Article

The Suitability of Methylene Blue Discoloration (MB Method) to Investigate the Fe^0/MnO_2 System

Viet Cao [1], Ghinwa Alyoussef [2], Nadège Gatcha-Bandjun [3], Willis Gwenzi [4] and Chicgoua Noubactep [2,5,6,*]

[1] Faculty of Natural Sciences, Hung Vuong University, Nguyen Tat Thanh Street, Viet Tri 35120, Phu Tho, Vietnam; caoviet@hvu.edu.vn
[2] Angewandte Geologie, Universität Göttingen, Goldschmidtstraße 3, D-37077 Göttingen, Germany; ghenwa_alyousef@yahoo.com
[3] Department of Chemistry, Faculty of Science, University of Maroua, BP 46 Maroua, Cameroon; nadegegatcha@yahoo.fr
[4] Biosystems and Environmental Engineering Research Group, Department of Soil Science and Agricultural Engineering, University of Zimbabwe, P.O. Box MP167, Mt. Pleasant, Harare, Zimbabwe; wgwenzi@yahoo.co.uk
[5] Centre for Modern Indian Studies (CeMIS), Universität Göttingen, Waldweg 26, 37073 Göttingen, Germany
[6] Department of Water and Environmental Science and Engineering, Nelson Mandela African Institution of Science and Technology, P.O. Box 447, Arusha, Tanzania
* Correspondence: cnoubac@gwdg.de

Abstract: The typical time-dependent decrease of the iron corrosion rate is often difficult to consider while designing Fe^0-based remediation systems. One of the most promising approaches is the amendment with manganese dioxide (Fe^0/MnO_2 system). The resulting system is a very complex one where characterization is challenging. The present communication uses methylene blue discoloration (MB method) to characterize the Fe^0/MnO_2 system. Shaken batch experiments (75 rpm) for 7 days were used. The initial MB concentration was 10 mg L^{-1} with the following mass loading: $[MnO_2]$ = 2.3 g L^{-1}, [sand] = 45 g L^{-1}, and $0 < [Fe^0]$ (g L^{-1}) ≤ 45. The following systems where investigated: Fe^0, MnO_2, sand, Fe^0/MnO_2, Fe^0/sand, and Fe^0/MnO_2/sand. Results demonstrated that MB discoloration is influenced by the diffusive transport of MB from the solution to the aggregates at the bottom of the test-tubes. Results confirm the complexity of the Fe^0/MnO_2/sand system, while establishing that both MnO_2 and sand improve the efficiency of Fe^0/H_2O systems in the long-term. The mechanisms of water decontamination by amending Fe^0-based systems with MnO_2 is demonstrated by the MB method.

Keywords: manganese oxides; MB method; reactivity materials; water treatment; zero-valent iron

check for updates

Citation: Cao, V.; Alyoussef, G.; Gatcha-Bandjun, N.; Gwenzi, W.; Noubactep, C. The Suitability of Methylene Blue Discoloration (MB Method) to Investigate the Fe^0/MnO_2 System. *Processes* **2021**, *9*, 548. https://doi.org/10.3390/pr9030548

Academic Editor: José A. Peres

Received: 22 February 2021
Accepted: 15 March 2021
Published: 19 March 2021

1. Introduction

The use of metallic iron (Fe^0) for environmental remediation and water treatment has boomed during the past three decades [1–3]. Under environmental conditions, Fe^0 is spontaneously oxidized to Fe^{II} and Fe^{III} oxides/hydroxides (iron corrosion products—FeCPs) which remove contaminants from an aqueous solution by adsorption and co-precipitation [4–7]. An inherent problem of Fe^0 is that its corrosion rate decreases with increasing service life [8]. This property has been termed as reactivity loss in the Fe^0 literature. Since the end of the 1990s, efficient tools have been sought to address "reactivity loss" or improve the corrosion rate. Tested approaches include [1,3]: increasing the specific surface area including using nano-Fe^0, alloying Fe^0 with more noble metals (e.g., Fe^0/Pd^0), adding oxidizing solutions (e.g., H_2O_2, O_3), and admixing with other aggregates (e.g., gravel, MnO_2, pyrite, sand). Except for MnO_2 addition, it is very difficult to maintain the enhanced Fe^0 oxidation effect for a long time. There are three main reasons: (i) added oxidizers are unstable solutions (e.g., H_2O_2), (ii) oxidation enhancers are in limited quantity (e.g., bimetallic coating), and (iii) the enhancing capacity of the aggregate is limited (e.g., gravel, sand). In contrary, the

addition of MnO_2 potentially creates a reactive Fe and Mn oxides mixture, for which long term reactivity is acknowledged but yet to be investigated [9,10].

Fe^0/MnO_2 systems have been extensively investigated during the past two decades and include: (i) Fe^0/MnO_2 composites [11,12] and (ii) Fe^0/MnO_2 mixtures [7,13]. There is an agreement on the MnO_2 enhancing decontamination effects in Fe^0/H_2O system, but reported disagreement on the actual operating mode of this system. Theoretically, MnO_2 can influence contaminant removal via adsorption, catalysis, and redox activities [14]. MnO_2 participates in oxidation of selected contaminants (e.g., aromatic amines, antibiotics). It can also function in a galvanic cell with iron to promote electron transfer on the surface of iron to alleviate Fe^0 passivation. The following three examples illustrate discrepancy in reports (i) Liang et al. [12] reported that there was no galvanic cells between Fe^0 and MnO_2 in Fe^0/MnO_2 composites for As removal. Rather, there is formation of a Fe/Mn binary oxides layer on the Fe^0 surface resulting in intensive corrosion. In other words, Liang et al. [12] argued that binary Fe/Mn oxides avoid or suppress the formation of crystalline iron (hydr)oxides. (ii) Gheju and Balcu [7] argued that the favorable synergistic effect of Fe^0/MnO_2 mixtures results from the capacity of MnO_2 to accelerate Fe^0 oxidative dissolution. Thereby, supplementary amounts of secondary adsorbents and reductants are generated for Cr^{VI} removal and reduction. (iii) Dong et al. [14] enhanced electron transfer "on the surface of Fe^0 with the presence of MnO_2" in the process of tetracycline removal, yielding a more sustainable Fe^0/H_2O system to lengthen the lives of the Fe^0 filtration system. There is an urgent need to clarify the real operating mode of the Fe^0/MnO_2 system.

This study seeks to clarify the operating mode of Fe^0/MnO_2 systems using the methylene blue discoloration method (MB method). The MB method entails characterizing MB discoloration in Fe^0/sand systems [15,16]. The Fe^0/MnO_2/sand system is characterized for MB discoloration for 7 days. A commercial Fe^0 specimen and a natural MnO_2 mineral are used. Three single (Fe^0, MnO_2, sand), two binary (Fe^0/MnO_2 and Fe^0/sand) and one ternary (Fe^0/MnO_2/sand) systems are investigated and the results are comparatively discussed.

2. The Fe^0/MnO_2 System

Aqueous contaminant removal in the presence of Fe^0 primary depends on the chemical thermodynamics of two redox systems: Fe^{II}/Fe^0 ($E^0 = -0.44$ V) and H^+/H_2O ($E^0 = 0.00$ V). Both aqueous solution behavior and redox thermodynamics should be considered. In addition, the eventual redox properties of contaminants (e.g., As, Cr, MB) and additives (e.g., Fe_3O_4, FeS_2, MnO_2) are to be equally considered. Table 1 summarizes the half-redox reactions relevant for the discussion in this paper and their electrode potential. As a rule, Fe^0 can be oxidized by the reducing agent of all couples with $E^0 > -0.44$ V.

Table 1. Electrode potentials of redox reactions relevant for the discussion in this study (modified after Reference [17]). MB^+ is the cationic methylene blue (MB), and LMB is its colorless reduced form.

Reaction	E^0 (V)	Number
$Fe^{2+} + 2\,e^- \Leftrightarrow Fe^0$	−0.44	(1)
$2\,H^+ + 2\,e^- \Leftrightarrow H_2$	0.00	(2)
$MB^+ + 2\,e^- + H^+ \Leftrightarrow LMB$	0.01	(3)
$Fe^{3+} + e^- \Leftrightarrow Fe^{2+}$	0.77	(4)
$O_2 + 2H_2O + 4\,e^- \Leftrightarrow 4OH^-$	0.81	(5)
$MnO_2 + 4H^+ + 2\,e^- \Leftrightarrow Mn^{2+} + 2H_2O$	1.23	(6)

The five theoretically possible redox reactions ($E^0 > -0.44$ V) are Fe^0 oxidation by: (i) water (H^+), (ii) methylene blue (MB^+), (iii) ferric iron (Fe^{3+}), (iv) dissolved oxygen (O_2), and (v) manganese dioxide (MnO_2). However, it has been clearly established that, at pH > 4.5 only water oxidized Fe^0 [18,19]. In other words, Fe^0 cannot be the anodic reaction

simultaneous to the reduction of MB^+, O_2 and MnO_2. Clearly, wherever these species have been reduced in a Fe^0/H_2O system, electron donors were primary (Fe^{II}, H_2) or secondary (Fe_3O_4, green rust) iron corrosion products. This knowledge is century old [2,18]. The major reason why electrons from Fe^0 are not available to dissolved species is that the Fe^0 surface is always covered by an oxide scale which acts as a diffusion barrier for dissolved species, and an electronic barrier for electrons. Concerning ferric ions (Table 1 (4)), it is considered that Fe^{3+} ions are generated in the vicinity of Fe^0 and may exchange electrons with the metal body. Clearly, the only two possible electrochemical reactions in a Fe^0/H_2O system are (Equations (1) and (2)):

$$Fe^0 + 2\,H^+ \Rightarrow Fe^{2+} + H_2 \quad (1)$$

$$Fe^0 + 2\,Fe^{3+} \Rightarrow 3\,Fe^{2+} \quad (2)$$

There are many possible reaction combinations emanating from Table 1. The discussion is limited on the fate of MB^+, MnO_2 and O_2, which are reactants in this study. The survey of the E^0 values reveals two key issues: (i) Fe^{3+} and MnO_2 oxidize LMB to MB^+, and (ii) O_2 and MnO_2 oxidize Fe^{2+}. In other words, MB discoloration by a redox process is not possible in the Fe^0/H_2O system, while the production of Fe^{III} species might be quantitative. Fe^{III} oxides are contaminant scavengers and in this study discoloring agents for MB [16]. Clearly, Fe^{2+} from iron corrosion (Table 1 (1)) is initially used to reduce MnO_2 (Equation (3)). Once the oxidative capacity of MnO_2 is exhausted, "excess" Fe^{III} oxides are generated for MB quantitative discoloration by adsorption and co-precipitation.

$$2\,Fe^{2+} + MnO_2 + 2\,H_2O \Rightarrow Mn^{2+} + 2\,FeOOH + 2\,H^+ \quad (3)$$

To summarize, the chemistry of the Fe^0/MnO_2 system shows two important features: (i) Fe^0 cannot exchange electrons with any dissolved species, and (ii) MnO_2 cannot form a galvanic cell with Fe^0. The remaining theoretical possibilities are: (i) MnO_2 influences contaminant removal via adsorption, catalysis, co-precipitation and redox activities (Assertion 1), (ii) MnO_2 participates in the oxidation of selected contaminants (Assertion 2), and (iii) MnO_2 disturbs the formation of oxide scales in the vicinity of Fe^0 (Assertion 3). Assertion 3 is obvious and universally valid as even external Fe^{2+} disturbs the formation of oxide scale [6,17]. The remaining task is to check the validity of Assertion 1 and Assertion 2 on a case specific basis. Herein, the discussion is eased by the evidence that MB has not adsorptive nor reductive affinities with the species in presence. In other words, MB discoloration results from co-precipitation with excess FeCPs. Adding sand to the system is inherent to the MB method [16], wherein the discoloration of MB by sand is inhibited as it is progressively coated by in-situ generated FeCPs. The validity of Assertion 1 and Assertion 2 will be tested for the $Fe^0/MnO_2/MB$ system.

3. Materials and Methods

This experimental section is adapted from Xiao et al. [20] using the same experimental design but quiescent experiments (0 rpm) and pyrite (FeS_2) as an additive.

3.1. Solutions

The used methylene blue (MB-Basic Blue 9 from Merck) was of analytical grade. The working solution was 10.0 mg L^{-1} prepared by diluting a 1000 mg L^{-1} stock solution. The stock solution was prepared by dissolving accurately weighted MB in tap water. The use of tap water rather than deionized water was motivated by the fact that tap water is closer to natural water in its chemical composition. The MB molecular formula is $C_{16}H_{18}N_3SCl$ corresponding to a molecular weight of 319.85 g. MB was chosen in this study because of its well-known strong adsorption onto solids [20].

3.2. Solid Materials

3.2.1. Metallic Iron (Fe^0)

The used Fe^0 material was purchased from iPutech (Rheinfelden, Germany). The material is available as filings with a particle size between 0.3 and 2.0 mm. Its elemental composition as specified by the supplier was: C: 3.52%; Si: 2.12%; Mn: 0.93%; Cr: 0.66% while the balance was Fe. The material was used without any further pre-treatment. Fe^0 was proven as a powerful discoloration agent for MB given that discoloration agents in the form of FeCPs are progressively generated in situ [20].

3.2.2. Manganese Dioxide (MnO_2)

The tested natural MnO_2-bearing minerals was Manganit from Ilfeld/Harz, Thüringen (Germany). The mineral was crushed and fractionated by sieving. The fraction 0.5–1.0 mm was used without any further pre-treatment. No chemical, mineralogical nor structural characterizations were performed. MnO_2 is a reactive mineral [21,22] and is used to delay the availability of "free" iron corrosion products (FeCPs) in the system. This results in a delay of quantitative MB discoloration [16].

3.2.3. Sand

The used sand was a commercial material for aviculture ("Papagaiensand" from RUT–Lehrte/Germany). The sand was used as received without any further pre-treatment. The particle size was between 2.0 and 4.0 mm. Sand was used as an adsorbent because of its worldwide availability and its use as admixing agent in Fe^0 barriers [23,24]. The adsorption capacity of sand for MB has been systematically documented as early as in 1955 by Mitchell et al. [25].

3.3. MB Discoloration

Shaken batch experiments at 75 rpm were conducted in assay tubes for an experimental duration of 7 d. The batches consisted of 0.0 or 1.0 g of sand, 0.0 to 0.1 g to Fe^0, 0.0 or 0.05 g of MnO_2 and mixtures thereof in 22.0 mL of a 10.0 mg L^{-1} MB solution. The six investigated systems were: (i) Fe^0 alone, (ii) sand alone, (iii) MnO_2 alone, (iv) Fe^0/sand, (v) Fe^0/MnO_2 and (vi) Fe^0/sand/MnO_2. The efficiency of individual systems at discoloring MB was characterized at laboratory temperature (about 22 °C). Initial pH was about 8.2. After equilibration, up to 3.0 mL of the supernatant solutions were carefully retrieved (no filtration) for MB measurements (no dilution). Each experiment was performed in triplicate, and averaged values are presented. Table 2 summarizes the aggregate content of the 6 Fe^0/MnO_2/sand systems investigated herein. The operational reference (blank experiment) is also added. Note that the pure Fe^0 system (Fe^0 alone) is regarded as a 'Fe^0/MnO_2/sand system', without MnO_2 nor sand.

Table 2. Overview of the six (6) investigated systems. The material loadings correspond to Figure 1.

System	Fe^0 (g L^{-1})	Sand (g L^{-1})	MnO_2 (g L^{-1})	Materials	Comments
Reference	0.0	0.0	0.0	None	Blank experiment
System 1	4.5	0.0	0.0	Fe^0 alone	Blank for Fe^0
System 2	0.0	45.0	0.0	Sand alone	Blank for sand
System 3	0.0	0.0	2.3	MnO_2 alone	Blank for MnO_2
System 4	4.5	45.0	0.0	Fe^0/sand	Reference system
System 5	4.5	0.0	4.5	Fe^0/MnO_2	Reference system
System 6	4.5 to 45	45.0	4.5	Fe^0/sand/MnO_2	Fe^0 loading as variable

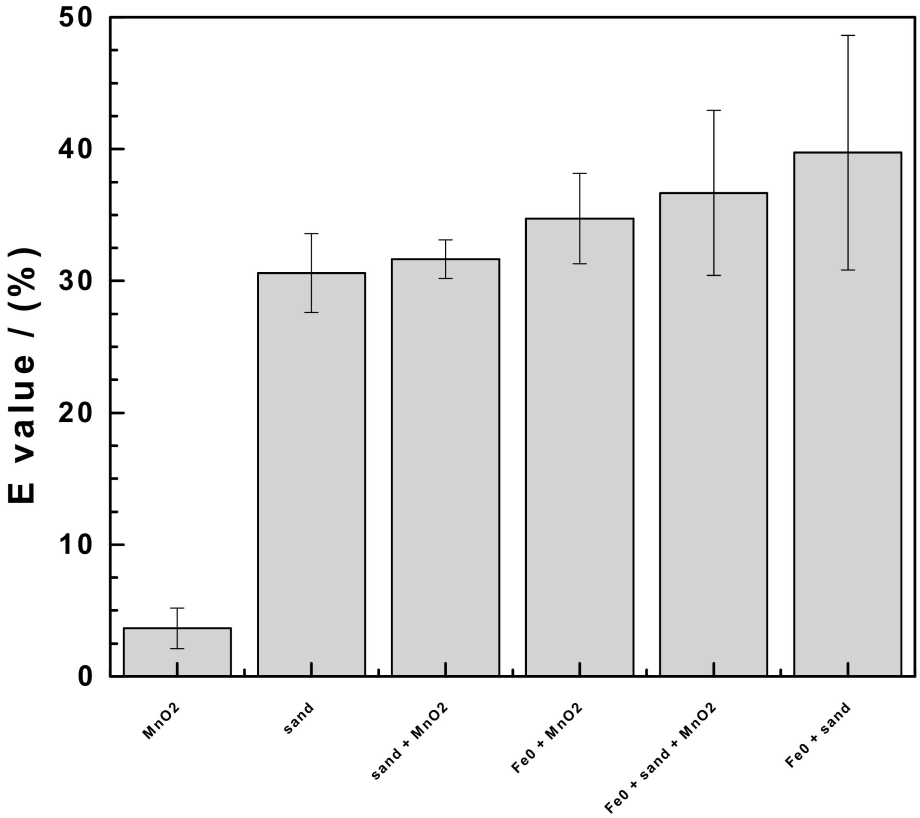

Figure 1. Comparison of the efficiency of tested materials for methylene blue (MB) discoloration for 7 days. Experimental conditions: [Fe^0] = 0 to 45 g L−1; [sand] = 45 g L−1; and [MnO_2] = 2.3 g L−1, shaken intensity: 75 rpm.

3.4. Analytical Methods

Iron and MB aqueous concentrations were determined by a Cary 50 UV-Vis spectrophotometer (Varian). The working wavelengths for MB and iron were 664.5 and 510.0 nm, respectively. Cuvettes with a 1.0 cm light path were used. The spectrophotometer was calibrated for Fe and MB concentrations ≤10.0 mg L^{-1}. The pH value was measured by combined glass electrodes (WTW Co., Oberbayern, Germany).

3.5. Expression of MB Discoloration Results (E Value)

In order to characterize the magnitude of the tested systems for MB discoloration, the discoloration efficiency (E) was calculated (Equation (4)). After the determination of the residual MB concentration (C), the corresponding percent MB discoloration (E value) was calculated as:

$$E = [1 - (C/C_0)] \times 100\% \quad (4)$$

Where, C_0 is the initial aqueous MB concentration (ideally 10.0 mg L^{-1}), while C gives the MB concentration after the experiment. The operational initial concentration (C_0) for each case was acquired from a triplicate control experiment without additive material (so-called blank). This procedure was to account for experimental errors during dilution of the stock solution, MB adsorption onto the walls of the reaction vessels, and all other possible side reactions during the experiments.

4. Results and Discussion

4.1. Evidence for the Complexity of the Fe^0/MnO_2 System

Figure 1 summarizes the extent of MB discoloration in the six investigated systems. It is seen that the pure MnO_2 system does not exhibit any significant MB discoloration

while the remaining systems exhibited E values varying from 30 to 40%. All these systems have in common the presence of sand (45.0 g L^{-1}) and those containing Fe^0, additionally contains 4.5 g L^{-1} of this reactive material. The evidence that adding 4.5 g L^{-1} of Fe^0 and 2.3 g L^{-1} of MnO_2 to 45.0 g L^{-1} sand does not significantly improve the extent of MB discoloration can be regarded as intriguing. Previous reports using quiescent batch experiments even reported on an initial decrease of E values in Fe^0/H_2O systems due to the presence of both MnO_2 and sand [16]. Clearly, while increasing the available surface area (different materials), MB discoloration is not initially improved. This can be justified by one or both of the following hypotheses: (i) chemical reactions occurring in the system hinder MB discoloration by adsorption onto sand (Hypothesis 1), and (ii) there are chemical interactions between available aggregates (e.g., Fe^0 and MnO_2) avoiding or delaying MB discoloration (Hypothesis 2). Hypothesis 1 corresponds to the historical observation by Mitchell et al. [25] that clean sand is a better adsorbent for MB that iron oxide-coated sand. This idea is also the cornerstone of the MB method and the reason why sand was added in the present study. Hypothesis 2 considers the reactive nature of MnO_2 [21,22] and encompasses the fact that by using Fe^{2+} for its reductive dissolution (Equation (3)), MnO_2 is delaying the availability of 'free' FeCPs for MB discoloration by co-precipitation [26].

Hypothesis 1: *Chemical reactions occurring in the system hinder MB discoloration by adsorption onto sand.*

Hypothesis 2: *There are chemical interactions between available aggregates (e.g., Fe^0 and MnO_2) avoiding or delaying MB discolor-ation.*

A closer look at Figure 1 reveals the following increasing order of E values: MnO_2 (3%) < sand (30%) < MnO_2/sand (31%) < Fe^0/MnO_2 (34%) < Fe^0/MnO_2/sand (36%) < Fe^0/sand (40%). Considering the standard deviations (Figure 1) it is clear that there was no significant difference between the performance of the three Fe^0-bearing systems: Fe^0/MnO_2 (34 ± 4%) < Fe^0/MnO_2/sand (36 ± 7%) < Fe^0/sand (40 ± 9%). Considering the absolute values, the ternary system (Fe^0/MnO_2/sand) performed less than the binary system with sand (Fe^0/sand). For binary systems, Fe^0/MnO_2 exhibited the lowest extent of MB discoloration. These observations collectively validate Hypothesis 2: MnO_2 reductive dissolution initially decreases the number of active sites for MB discoloration. This is because Fe^{2+} oxidation (Equation (3)) occurs at the MnO_2 surface and resulting Fe^{III} oxides coat the MnO_2 surface and is thus not available for the co-precipitation of the cationic dye (MB).

The remainder of the presentation discusses changes in the ternary Fe^0/MnO_2/sand system as the Fe^0 loading varies from 0 to 45 g L^{-1} while the sand loading is 45 g L^{-1} and the MnO_2 loading 2.3 g L^{-1}.

4.2. MB Discoloration

Figure 2 summarizes changes of the E values in the systems Fe^0/MnO_2, Fe^0/sand, and Fe^0/MnO_2/sand as the Fe^0 loading varied from 0 to 45 g L^{-1}. It is seen that at [Fe^0] = 0 g L^{-1}, the two sand-bearing systems exhibited an E value close to 30%. This corresponds to the results reported in Figure 1 and is in tune with the observation of Mitchell et al. [25], that sand is an excellent adsorbent for MB [15,16]. It is also seen that the E value monotonously increases with increasing Fe^0 loadings reaching a maximum value of about 52% for the Fe^0/sand system and 64% for the ternary system respectively. The observation that the ternary system performed better than the binary may be misunderstood as contrary to the reports in Section 1 (Figure 1). However, data in Figure 1 corresponds to [Fe^0] = 4.5 g L^{-1}. Figure 2 clearly shows that for this Fe^0 loading, Fe^0/sand performs better than Fe^0/MnO_2/sand. The better performance of the ternary system relative to Fe^0/sand for [Fe^0] > 10 g L^{-1}, is attributed to the action of MnO_2 in reinforcing Fe^0 corrosion and producing "excess" FeCPs for MB co-precipitation. This operating mode is illustrated the

best in the binary Fe^0/MnO_2 system which performed lower that the sand-bearing systems for $[Fe^0] < 10$ g L^{-1}, and far higher for $[Fe^0] > 10$ g L^{-1}, reaching 70% at $[Fe^0] = 45$ g L^{-1}.

The Fe^0/MnO_2 system shows a diphasic pattern in the process of MB discoloration. The initial discoloration (up to $[Fe^0] = 12$ g L^{-1}) is very rapid, followed by slower discoloration for higher $[Fe^0]$ values. It can be considered that for $[Fe^0] < 12$ g L^{-1}, the Fe^0/MnO_2 ratio is optimal to avoid intra-particle diffusion such that "excess" FeCPs is immediately available for MB co-precipitation. For $[Fe^0] > 12$ g L^{-1}, MB must diffuse through a thicker layer of Fe^0 particles at the bottom of the test-tubes. Remember that in the presence of sand, the diffusion paths are larger and explain why, for higher Fe^0 loadings, the ternary system performed less than the Fe^0/MnO_2 system, despite initial rapid adsorption onto sand. In other words, after the complete coverage of sand by FeCPs, MB discoloration solely results from co-precipitation with free FeCPs. These free FeCPs are less available in the ternary system compared to the binary Fe^0/MnO_2 system.

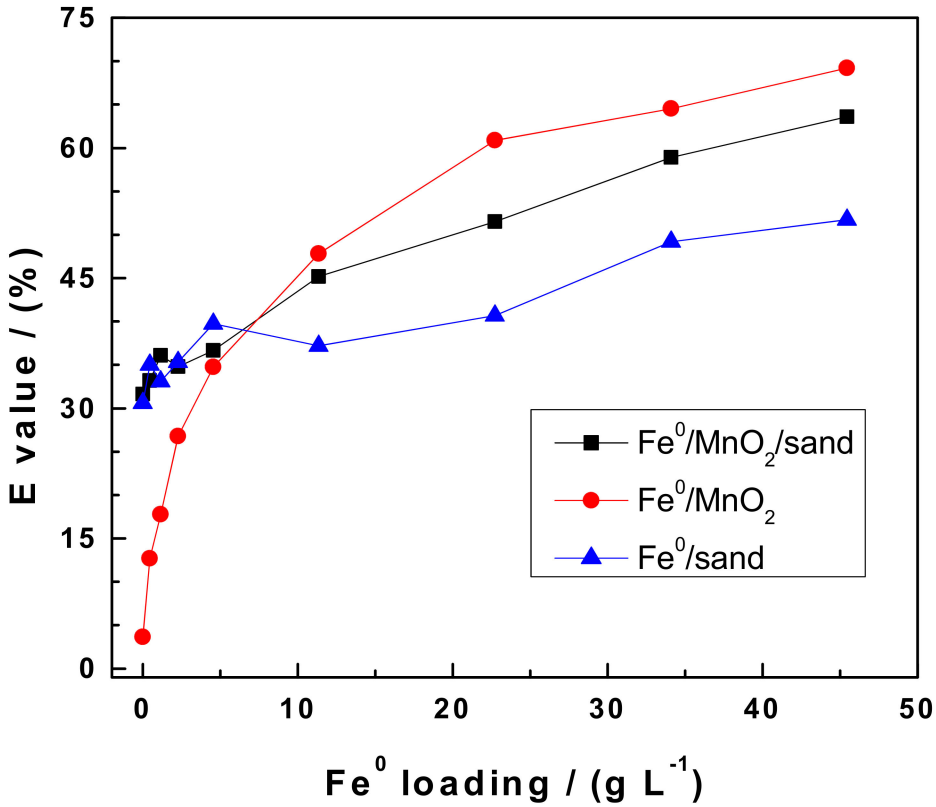

Figure 2. Methylene blue discoloration in Fe^0/sand/MnO_2 systems as impacted by the addition of various Fe^0 loading for 7 days. Experimental conditions: $[Fe^0] = 2.3$ to 45 g L−1; [sand] = 45 g L−1; and $[MnO_2] = 2.3$ g L−1, shaken intensity: 75 rpm. The lines are not fitting functions, they simply connect points to facilitate visualization.

4.3. pH Value

Figure 3 summarizes changes of the pH values in the systems Fe^0/MnO_2, Fe^0/sand, and Fe^0/MnO_2/sand as the Fe^0 loading varied from 0 to 45 g L^{-1} ($pH_0 = 8.2$). It is seen that for $[Fe^0] < 10$ g L^{-1}, the three systems exhibited very different behaviors; the pH value (i) first decreased to a minimum of 7.8 for $[Fe^0] = 2.3$ g L^{-1} in the Fe^0/MnO_2/sand system, (ii) is constant to 8.1 in the Fe^0/sand system, and (iii) monotonously increased in the Fe^0/MnO_2 system. The two processes determining the final pH value in each systems are: (i) iron corrosion consuming protons (Equation (1)), and MnO_2 reductive dissolution releasing protons (Equation (3)). Accordingly, in the Fe^0/sand system, only iron corrosion fixes the pH and the constant value for $[Fe^0] < 11$ g L^{-1} corresponds to H^+ adsorption onto

the surface of sand. The pH starts to increase only after the ion exchange capacity of sand for H^+ is exhausted.

Concerning the Fe^0/MnO_2 system, there was a slight pH decrease for $[Fe^0]$ = 0.5 and 1.1 g L^{-1} but from $[Fe^0]$ = 2.3 g L^{-1} onwards, there was an increase of the pH value. This means that under the experimental conditions (e.g., used mass loading and shaken at 75 rpm for 7 days), MnO_2 reductive dissolution fixed the final pH value only for $[Fe^0] < 2.3$ g L^{-1}. For higher Fe^0 loadings, the pH is fixed by iron corrosion and the final pH values determined by the extent to which free protons are released to the solution above the mixture of aggregates (e.g., Fe^0, MnO_2 and sand). For this reason, the Fe^0/MnO_2 (without sand) exhibited larger final pH values than the Fe^0/MnO_2/sand in which protons are fixed at the negatively charged sand surface.

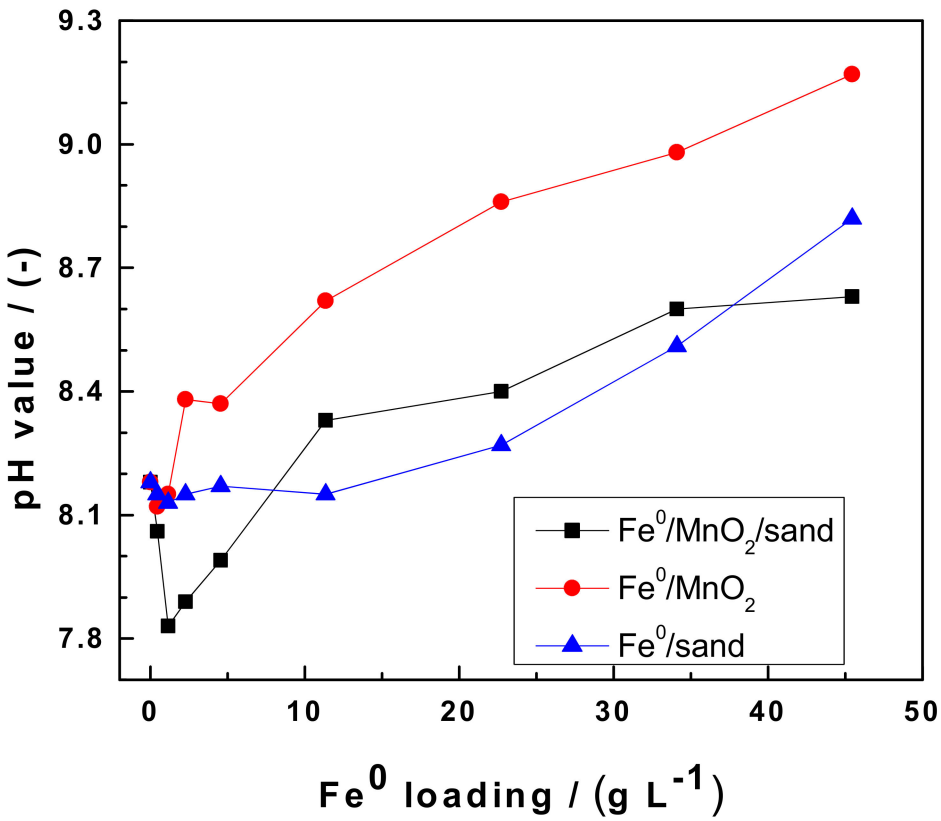

Figure 3. pH value in Fe^0/sand/MnO_2 systems as impacted by the addition of various Fe^0 loading for 7 days. Experimental conditions: $[Fe^0]$ = 2.3 to 45 g L−1; [sand] = 45 g L−1; and $[MnO_2]$ = 2.3 g L−1, shaken intensity: 75 rpm. The lines are not fitting functions, they simply connect points to facilitate visualization.

4.4. The Operating Mode of Fe^0/MnO_2 Systems

The efficiency of Fe^0/H_2O systems for water decontamination relies primarily on the electrochemical corrosion of Fe^0 by water (Equation (1)). This oxidative dissolution is followed by a series of chemical reactions in the vicinity of the Fe^0 surface yielding to the formation of an oxide scale which is known as passive film [1,3]. The enhanced efficiency of $Fe^0/MnO_2/H_2O$ systems compared to their Fe^0/H_2O counterparts has been correctly justified by sustained generation of native FeCPs for contaminant adsorption and co-precipitation. However, the further interpretation of achieved results were species-dependent. For example, Bui et al. [26] considered that there are oxidative species like OH radicals in the system to oxidize As^{III} to As^{V} with better adsorptive affinities to FeCPs. This explanation becomes speculative when one considers that quantitative removal of Se which has also been documented [27], premised the reduction of Se^{VI} to Se^{VI}. By using MB

as operational tracer for the availability of FeCPs in investigated systems, this study has elegantly explained the operating mode of the $Fe^0/MnO_2/H_2O$ system.

By adding sand to the system as per the MB method [15,16], this study has thoroughly characterized MB discoloration in the Fe^0/MnO_2/sand/H_2O system. Changes of the E and pH values clearly show that sand is coated in situ by FeCPs and thus, can be regarded as storage room for fresh FeCPs, avoiding their accumulation in the Fe^0 vicinity and thus, delaying Fe^0 passivation. Fe^0 passivation is also delayed by two major factors attributed to the presence of MnO_2: (i) consumption of Fe^{2+} for the MnO_2 reductive dissolution (Equation (3)) [28], and (ii) disturbance of the generation of "protective" oxides by virtue of the presence of Mn^{2+} ions.

The discussion of the chemistry of the $Fe^0/MnO_2/H_2O$ systems has excluded the formation of galvanic cells between Fe^0 and MnO_2 as a reason for enhanced efficient of Fe^0/H_2O systems through MnO_2 amendment. Given that the reductive transformation of any dissolved species by electrons from the metal body is impossible [18,19,29], this study established that adding MnO_2 to Fe^0/H_2O systems should be regarded as creating a reactive Fe/Mn mineral mixture. The geochemistry of such mixtures is well-known to geochemists [9,10,30,31]. However, their suitability for decontaminating engineered systems is yet to be systematically investigated [30,31].

Finally, the working hypotheses shall be tested: (i) MnO_2 influences contaminant removal via adsorption, catalysis, co-precipitation and redox activities (Assertion 1), and MnO_2 participates in the oxidation of selected contaminants (Assertion 2). Both assertions are valid as the MB method is just like a "separation of variables" enabling to trace the availability of native FeCPs which are Fe minerals. The mixture of Fe and Mn minerals is a reactive system that shall be tested for several contaminants and groups of contaminants to prepare for the advent of sustainably engineered Fe^0/MnO_2 systems.

5. Conclusions

The MB method proved to accurately describe the complexity of the Fe^0/MnO_2/sand system. In particular, despite the absence of chemical, mineralogical/structural and morphological characterization of used aggregates, this method sufficiently described the dynamics within the named system. The uniqueness of the MB method is its simplicity and its affordability as only a UV sprectrophotometer is needed. The method can be adapted to all Fe^0-based systems. However, it should be carefully considered that site-specific experiments with relevant contaminants are still unavoidable. This is because the affinity of individual contaminants to FeCPs depends on its speciation as well. The major output of this research is that MnO_2 sustains Fe^0 corrosion and thus the decontamination efficiency of Fe^0/H_2O systems. Thus adding, calculated amounts of well-characterized MnO_x minerals to Fe^0 filters is one highway to more sustainable filtration systems. In exploring this avenue, the reactivity of used aggregates should receive particular attention.

Author Contributions: G.A., V.C., N.G.-B. and C.N. conceived the presented idea and developed the theory. G.A. carried out the experiment. C.N. supervised this work. W.G. supervised the redaction of the first draft by V.C. and N.G.-B. All authors discussed the results and contributed to the final manuscript. All authors have read and agreed to the published version of the manuscript.

Funding: This research received no external funding.

Institutional Review Board Statement: Not applicable.

Informed Consent Statement: Not applicable.

Data Availability Statement: Not applicable.

Acknowledgments: For providing the iron material investigated in this study the authors would like to express their gratitude to iPutec GmbH (Rheinfelden, Germany). The natural MnO_2-mineral was provided by the Department of Geology of the Technical University Bergakademie Freiberg/Germany (Mineralsammlung). The manuscript was improved by the insightful comments of anonymous

reviewers from Processes. We acknowledge support by the German Research Foundation and the Open Access Publication Funds of the Göttingen University.

Conflicts of Interest: The authors declare no conflict of interest.

References

1. Guan, X.; Sun, Y.; Qin, H.; Li, J.; Lo, I.M.C.; He, D.; Dong, H. The limitations of applying zero-valent iron technology in contaminants sequestration and the corresponding countermeasures: The development in zero-valent iron technology in the last two decades (1994–2014). *Water Res.* **2015**, *75*, 224–248. [CrossRef] [PubMed]
2. Antia, D.D.J. Water treatment and desalination using the eco-materials n-Fe0 (ZVI), n-Fe_3O_4, n-$Fe_xO_yH_z$[mH_2O], and n Fe_x[Cation]nO_yH_z[Anion]m [rH_2O]. In *Handbook of Nanomaterials and Nanocomposites for Energy and Environmental Applications*; Kharissova, O.V., Ed.; Springer Nature: Berlin/Heidelberg, Germany, 2020.
3. Thakur, A.K.; Vithanage, M.; Das, D.B.; Kumar, M. A review on design, material selection, mechanism, and modelling of permeable reactive barrier for community-scale groundwater treatment. *Environ. Technol. Innov.* **2020**, *19*, 100917. [CrossRef]
4. Noubactep, C. Processes of contaminant removal in "Fe^0–H_2O" systems revisited. The importance of co-precipitation. *Open Environ. Sci.* **2007**, *1*, 9–13. [CrossRef]
5. Bojic, A.L.; Bojic, D.; Andjelkovic, T. Removal of Cu^{2+} and Zn^{2+} from model wastewaters by spontaneous reduction–coagulation process in flow conditions. *J. Hazard. Mater.* **2009**, *168*, 813–819. [CrossRef]
6. Ghauch, A. Iron-based metallic systems: An excellent choice for sustainable water treatment. *Freib. Online Geosci.* **2015**, *32*, 1–80.
7. Gheju, M.; Balcu, I. Sustaining the efficiency of the Fe(0)/H_2O system for Cr(VI) removal by MnO_2 amendment. *Chemosphere* **2019**, *214*, 389–398. [CrossRef] [PubMed]
8. Melchers, R.E.; Petersen, R.B. A reinterpretation of the Romanoff NBS data for corrosion of steels in soils. *Corros. Eng. Sci. Technol.* **2018**, *53*, 131–140. [CrossRef]
9. Huang, J.; Zhang, H. Redox reactions of iron and manganese oxides in complex systems. *Front. Environ. Sci. Eng.* **2020**, *14*, 76. [CrossRef]
10. Michel, M.M.; Reczek, L.; Papciak, D.; Włodarczyk-Makuła, M.; Siwiec, T.; Trach, Y. Mineral materials coated with and consisting of MnO_x—Characteristics and application of filter media for groundwater treatment: A review. *Materials* **2020**, *13*, 2232. [CrossRef] [PubMed]
11. Hussam, A.; Munir, A.K.M. A simple and effective arsenic filter based on composite iron matrix: Development and deployment studies for groundwater of Bangladesh. *J. Environ. Sci. Health A* **2007**, *42*, 1869–1878. [CrossRef] [PubMed]
12. Liang, Y.; Min, X.; Chai, L.; Wang, M.; Liyang, W.; Pan, Q.; Okido, M. Stabilization of arsenic sludge with mechanochemically modified zero valent iron. *Chemosphere* **2017**, *168*, 1142–1151. [CrossRef]
13. Burghardt, D.; Kassahun, A. Development of a reactive zone technology for simultaneous in situ immobilisation of radium and uranium. *Environ. Geol.* **2005**, *49*, 314–320. [CrossRef]
14. Dong, G.; Huang, L.; Wu, X.; Wang, C.; Liu, Y.; Liu, G.; Wang, L.; Liu, X.; Xia, H.; Dong, G. Effect and mechanism analysis of MnO_2 on permeable reactive barrier (PRB) system for the removal of tetracycline. *Chemosphere* **2018**, *193*, 702–710. [CrossRef] [PubMed]
15. Btatkeu-K, B.D.; Olvera-Vargas, H.; Tchatchueng, J.B.; Noubactep, C.; Caré, S. Characterizing the impact of MnO_2 on the efficiency of Fe^0-based filtration systems. *Chem. Eng. J.* **2014**, *250*, 416–422. [CrossRef]
16. Miyajima, K.; Noubactep, C. Characterizing the impact of sand addition on the efficiency of granular iron for water treatment. *Chem. Eng. J.* **2015**, *262*, 891–896. [CrossRef]
17. Alyoussef, G. Characterizing the Impact of Contact Time in Investigating Processes in Fe^0/H_2O Systems. Master's Thesis, University of Göttingen, Göttingen, Germany, 2016.
18. Whitney, W.R. The corrosion of iron. *J. Am. Chem. Soc.* **1903**, *25*, 394–406. [CrossRef]
19. Stratmann, M.; Müller, J. The mechanism of the oxygen reduction on rust-covered metal substrates. *Corros. Sci.* **1994**, *36*, 327–359. [CrossRef]
20. Xiao, M.; Cui, X.; Hu, R.; Gwenzi, W.; Noubactep, C. Validating the Efficiency of the FeS2 Method for Elucidating the Mechanisms of Contaminant Removal Using Fe^0/H_2O Systems. *Processes* **2020**, *8*, 1162. [CrossRef]
21. Appelo, C.A.J.; Postma, D. A consistent model for surface complexation on birnessite (-MnO_2) and its application to a column experiment. *Geochim. Cosmochim. Acta* **1999**, *63*, 3039–3048. [CrossRef]
22. Post, J.E. Manganese oxide minerals: Crystal structures and economic and environmental significance. *Proc. Natl. Acad. Sci. USA* **1999**, *96*, 3447–3454. [CrossRef]
23. Varlikli, C.; Bekiari, V.; Kus, M.; Boduroglu, N.; Oner, I.; Lianos, P.; Lyberatos, G.; Icli, S. Adsorption of dyes on Sahara desert sand. *J. Hazard. Mater.* **2009**, *170*, 27–34. [CrossRef] [PubMed]
24. Ndé-Tchoupé, A.I.; Makota, S.; Nassi, A.; Hu, R.; Noubactep, C. The Suitability of Pozzolan as Admixing Aggregate for Fe0-Based Filters. *Water* **2018**, *10*, 417. [CrossRef]
25. Mitchell, G.; Poole, P.; Segrove, H.D. Adsorption of methylene blue by high-silica sands. *Nature* **1955**, *176*, 1025–1026. [CrossRef]
26. Bui, T.H.; Kim, C.; Hong, S.P.; Yoon, J. Effective adsorbent for arsenic removal: Core/shell structural nano zero-valent iron/manganese oxide. *Environ. Sci. Pollut. Res.* **2017**, *24*, 24235–24242. [CrossRef]

27. Qin, H.; Sun, Y.; Yang, H.; Fan, P.; Qiao, J.; Guan, X. Unexpected effect of buffer solution on removal of selenite and selenate by zerovalent iron. *Chem. Eng. J.* **2018**, *334*, 296–304. [CrossRef]
28. Sanjeev, B.; Malay, C. Removal of arsenic from ground water by manganese dioxide-coated sand. *J. Environ. Eng.* **1999**, *125*, 782–784.
29. Noubactep, C. Metallic iron for environmental remediation: A review of reviews. *Water Res.* **2015**, *85*, 114–123. [CrossRef]
30. Brock, S.L.; Duan, N.; Tian, Z.R.; Giraldo, O.; Zhou, H.; Suib, S.L. A review of porous manganese oxide materials. *Chem. Mater.* **1998**, *10*, 2619–2628. [CrossRef]
31. Dong, G.; Han, R.; Pan, Y.; Zhang, C.; Liu, Y.; Wang, H.; Ji, X.; Dahlgren, R.A.; Shang, X.; Chen, Z.; et al. Role of MnO_2 in controlling iron and arsenic mobilization from illuminated flooded arsenic-enriched soils. *J. Hazard. Mater.* **2021**, *401*, 123362. [CrossRef]